Surface-Blowing Anti-Icing Technique for Aircraft Surfaces

A. H. Tabrizi*
Indiana Institute of Technology, Fort Wayne, Indiana
and
W. S. Johnson†
University of Tennessee, Knoxville, Tennessee

An experimental evaluation of surface blowing as an anti-icing technique applicable to aircraft surfaces is presented. A circular cylinder was used to approximate the leading edge of an aircraft icing surface utilizing a number of slots located at the frontal surface along the cylinder to inject air counter to the main air-droplet stream. The effects of air blowing for single and multiple slots as well as the effect of air injection rates on the reduction of ice accretion rate are reported. The experimental results indicate that surface blowing produces a general reduction in ice buildup.

Introduction

THE atmospheric icing environment, when encountered by an aircraft in flight, causes a number of operational and technical problems. The flight path of an unattended aircraft, such as a missile, can be drastically altered due to the ice accretion on its surfaces, jeopardizing mission success. The increase in drag of a helicopter blade due to ice buildup results in a high-torque rise of the propeller shaft, and ice shed from the leading edge of an engine inlet when ingested may cause structural damage to the internal parts of the engine. Safety considerations cause concern as to the probability of encountering icing conditions during a flight, the severity of these conditions, the effect if ice buildup on the performance of the aircraft both during and after the icing encounter, and the effectiveness of anti-icing or deicing techniques if ice formation is intolerable.

Icing can occur when an aircraft enters an atmospheric condition containing supercooled water droplets. Under such conditions, when a supercooled water droplet strikes the surface, ice is formed and adheres to the surface. The two types of accreted ice formations that commonly appear on airfoils are rime ice and glaze ice, as illustrated in Fig. 1.

Glaze ice generally forms under conditions of high air temperature (relative to the freezing temperature) and high liquid water content (conventionally expressed as g of water/m^3 of air volume). The freezing mechanism of glaze ice formation is as follows:

1) Droplets collected on the surface freeze from the bottom while growing in size by capturing smaller droplets from the air.

2) Once the aerodynamic drag forces on the droplets exceed the surface tension forces, water in the unfrozen portion of the droplets is swept away and freezes along the surface, producing horn-shaped glaze ice.

The freezing process for this case is very complex and believed to be highly dependent upon the air speed. Rime ice, on the other hand, is produced when highly supercooled water droplets strike the surface and freeze on impact without any runback.

Received Dec. 29, 1987.

*Assistant Professor, Department of Engineering. Member AIAA.

†Professor, Department of Mechanical Engineering.

Over the years a number of experimental and theoretical investigations have been conducted[1–6] to obtain insight into the mechanism of the ice accretion process and to predict the ice accretion rate. Numerical solutions of the flow over ice accretion shapes have also been reported.[7,8] Ice protection techniques have been developed and are catagorized as anti-icing (i.e., prevention of ice formation) and deicing (i.e., the periodic removal of ice already formed on the surface).

Examples of anti-icing techniques are the surface coating (hydrophobic surfaces) and chemical processes that are used to prevent the ice from adhering to the surface. Continuous heating of the surface was considered by Nichols.[9] He investigated the heat flux requirements to produce an ice-free leading edge of the engine inlet for cruise missiles with a strip heater configuration. His experimental results conducted in an icing wind tunnel suggest that an effective electrical anti-icing system can be achieved with a 12.5 W/in.^{2} power input into the heaters. The surface heating concept can be used both as an anti-icing and a deicing system. When used as a deicer, ice is allowed to collect on the surface for a period of time and then power is applied to the heaters. Operating this system as a deicer requires some judgment as to when to turn on the heaters, because if there is too much ice collected on the surface, deicing may not be possible. A glycol-exuding, porous, leading-edge ice protection system has been experimentally investigated by NASA Lewis Research Center[10] and British aircraft industries using a concept developed by TKS (Aircraft De-Icing) Limited of Great Britain.[11] This system

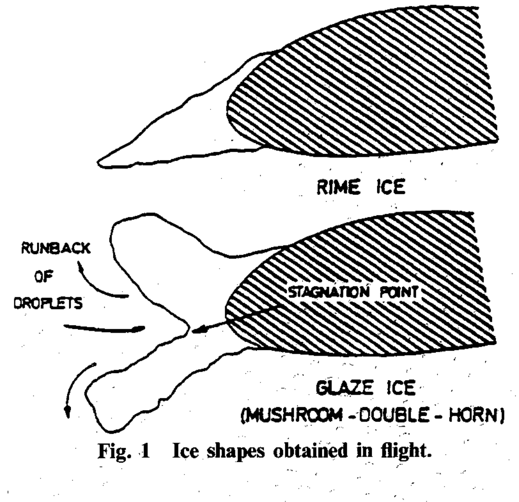

Fig. 1 Ice shapes obtained in flight.

can be operated in a deicing mode as well as in an anti-icing mode. It has been employed on numerous British aircraft with a high degree of success. Another deicing system includes inflatable pneumatic boots ("rubber shoes") that cover the leading edge and are periodically inflated and deflated, resulting in breakup of the ice layer and its subsequent shedding. At the present time, pneumatic boots are the only ice protection system employed on wings of light aircraft. While the success of this system has been demonstrated over the years it has been in use, there are some disadvantages: 1) some ice may remain on the surface during the breakup and shedding process; 2) premature actuation of the boot may only displace the ice without removing it, making further removal difficult; and 3) the boots are relatively expensive and must be replaced periodically.

Intermittent heating of airfoils utilizing hot air is considered theoretically by Hauger.[12] In this system, deicing of the surface was accomplished by bleeding hot air from the engine and allowing it to pass chordwise through double-skin passages in the wing. No experimental evidence of the success of this deicing system was found by the authors. An experimental and numerical investigation of an electrothermal deicer pad was performed by Leffel.[13] The deicer pad in this system is made of a composite structure that consists of a layer of insulation, a heating element, a second layer of insulation, and a layer of sheet metal as a shield. The deicer pad attaches directly to the wing surface. Even though the possibility of deicing by this system has been demonstrated, its feasibility and practicality remain to be established.

Another type of heater made from graphite composite material was investigated for potential deicing application by Hung et al.[14] The heating element in this system is a graphite fiber-epoxy composite, which is claimed to have very high electrical and thermal conductivity. The heater can conform to irregular surfaces because it can be made very thin. This heater is used with a fabric glass-epoxy as the protecting layer and is claimed to have a stronger bond to the protecting layer than the conventional metal foil heater. Wind-tunnel icing experiments utilizing this heater are needed to evaluate its deicing characteristics.

Ciardullo et al.[15] reported on the use of glass-capillary reinforced advanced composite structures for anti-icing purposes. The concept involves ducting heated air through glass capillary tubes embedded on the surface of a composite structure. Surface heating characteristics of this system were investigated, but it has not yet been tested in icing conditions.

This paper presents an experimental investigation of another technique[16,17] in which anti-icing is achieved by surface slot blowing. The air injection is intended to modify the effective shape of the icing surface, i.e., to displace the streamlines about the surface, thus altering the trajectories of droplets approaching the surface. These displaced trajectories result in reduction of the droplet collection rate on the surface. The extent of reduction in the ice accretion rate due to the surface blowing is then determined by measuring the weight of ice collected on the surface under a variety of blowing rates and other conditions.

This concept lends itself well to jet aircraft anti-icing because of an adequate supply of air at high pressure and temperature. In addition to the slot-blowing effect, the surface heating caused by the injection of high-temperature air further inhibits the formation of ice.

No attempt has yet been made to evaluate the effect of slot blowing on overall aerodynamic performance. Such a study will be very significant, however, in the total evaluation of this concept.

Experimentation

An experimental study was carried out to determine the effect of surface injection on the ice accretion rate on a circular cylinder (approximating the leading edge of an engine inlet, etc.). An open-circuit wind tunnel fitted with a pneumatic spray system was used in the experiments; the tunnel test section was circular, 12.5 in. in diameter, and 14 in. long. The primary parameter of interest to be determined was the ice collection rate on the cylinder for a variety of surface-blowing rates. The ice accretion rate was determined by freezing the water on the cylinder and weighing the ice formed during a certain period of time. Since the intent of the present investigation was not to simulate the ice shapes obtained under atmospheric icing conditions but rather to evaluate the effect of the surface injection on the collection rate, the actual freezing mechanism/process of droplets collected on the surface was not simulated. In the present experiments, the freezing of the water on the surface was accomplished by cooling the cylinder surface by continuously circulating chilled methanol (-30 to -45°F) through it.

Spray System

Water at about 35°F was sprayed into the wind tunnel using external mixing-type pneumatic atomizing nozzles. Figure 2 presents details of the spray system used in the tunnel. Spray nozzles were located approximately 5 ft upstream of the test section, and flow rate through each nozzle was approximately equal, as shown in Table 1.

Droplet size distribution produced by the pneumatic nozzles used in the experiments was determined as follows. A microscope slide was coated with a thin film of petroleum jelly and inserted into the flowfield at the test section. The diameters of droplets collected on the slide were then measured under a microscope, and the mean droplet diameter in the spray was calculated, producing the droplet size distribution data shown in Fig. 3. The mean droplet diameter in the spray at the test section was 45 μ.

Experimental Model

A model was built to study the feasibility and performance of the proposed anti-icing technique. The model consisted of

Table 1 Nozzle water flow rate calibration data and tunnel LWC

		Tunnel liquid water content^c × 10^3			
p^a	m^b × 10^3	$V^d = 4.1$	6.3	13.3	39
48	2.893	0.9	0.58	0.28	0.09
40	2.554	0.79	0.52	0.24	0.08
30	2.025	0.63	0.41	0.19	0.07
20	1.792	0.56	0.36	0.17	0.06
10	1.410	0.44	0.28	0.13	0.05

^{a}Nozzle air pressure, psig. ^{b}Nozzle water mass flow rate, lbm/s. ^{c}LWC, lbm/ft^3 of air. ^{d}Tunnel air velocity, ft/s.

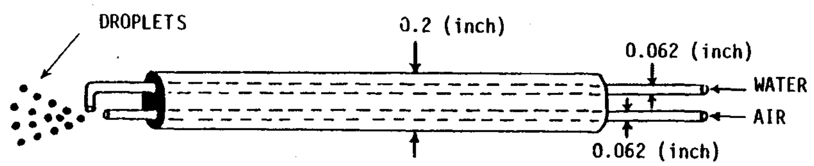

Fig. 2 Schematic of a pneumatic atomizing nozzle.

a circular cylinder made of 0.969-in.-o.d. brass tubing with three air injection slots located at 0, +50, and −50 deg, where 0 deg represented the front stagnation point. It should be noted that the angles at which slots were located on either side of the front stagnation point were optimized for manufacturing considerations and were not necessarily optimum for the anti-icing process. The injection slots were 4 in. long and 0.014 in. wide, and gaseous nitrogen was delivered to each of them through a 0.25-in.-diam copper tube. Air could not be used as an injectant due to condensation of moisture from the air and ice formation in the slots, even at very low humidity ratios. Dimensional details of the model are shown in Fig. 4.

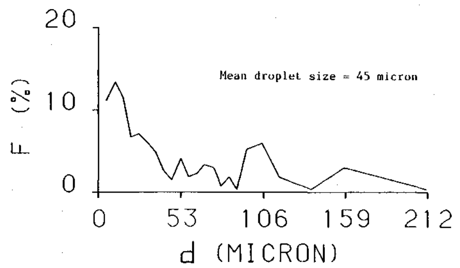

Fig. 3 Frequency of occurrence of a droplet size in the spray.

Figure 5 presents a schematic of the coolant and nitrogen supply systems used in the experiments.

Experimental Procedure/Results

To evaluate the effect of the surface injection on the ice accretion rate, a series of experiments was performed. A quantitative evaluation was performed by measuring the weight of ice collected on the model, while a qualitative evaluation was performed by comparing the profiles obtained from the ice layer buildup on the model.

The model was first tested with no surface injection of tunnel speeds of 4.1, 6.3, 13.3, and 39 ft/s. The amount of ice collected on the model was determined by weighting using a total run time of 7 min for each test. In all tests the mass of water injected into the tunnel through the spray system was maintained at 7.29 lbm/h. The total weight of collected ice for each case is presented in Tables 2 and 3. Figures 6–9 show the axial ice profiles at +5 deg from the front stagnation point, and the angular ice profiles at the center of the tunnel and at locations 1.25 in. away from the center on both sides. These profiles were obtained using a specially constructed constructed profilometer.[16]

The icing of the model with surface injection was considered next. Numerous tests were performed to investigate the

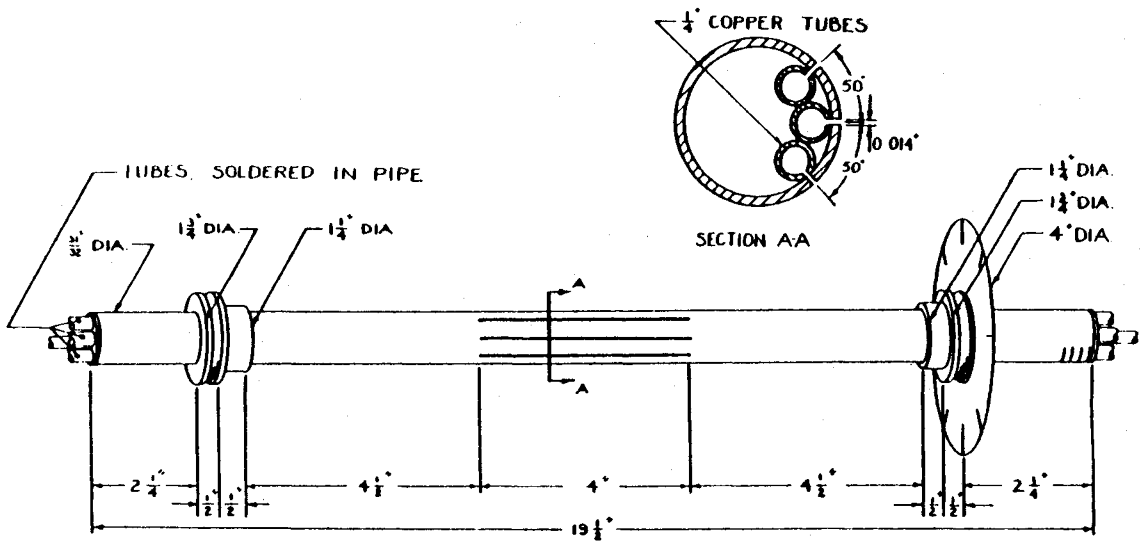

Fig. 4 Dimensional details of the experimental model.

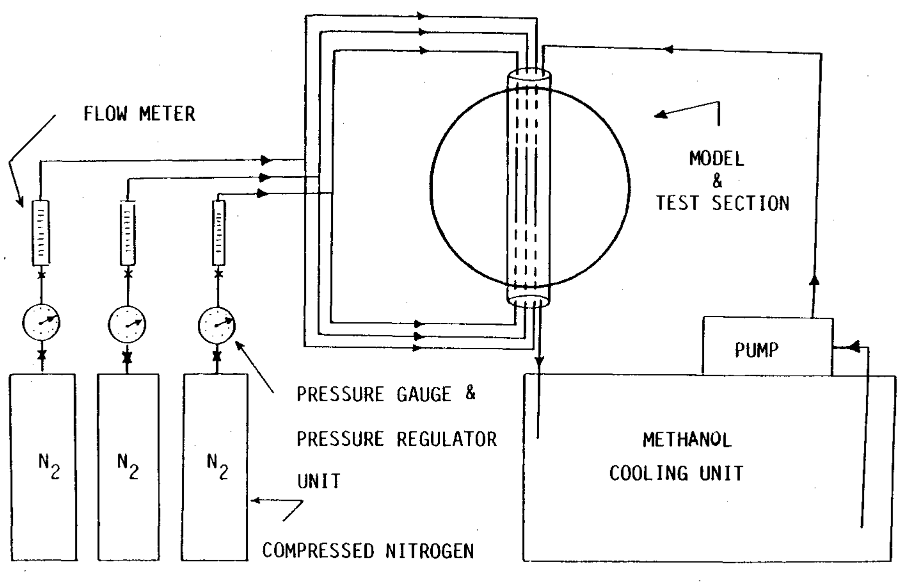

Fig. 5 Schematic of the cooling and nitrogen supply system.

effects of the number of slots on the model, as well as the injection rate through each slot. First, the effect of slot flow rate on the reduction of the ice collection was considered using a total of three slots located at 0, +50, and −50 deg from the front stagnation point with the flow through each slot set at 25 ft^3/h. The ice weight collected on the 4-in.-long blowing section of the model for 7 min of exposure at tunnel velocity of 6.3 ft/s was 3.17 g, compared to 4.92 g without slot injection. An increase in the flow rate through each slot to 100 ft^3/h with all other parameters kept constant produced an ice weight of 2.92 g. (These results were computed from the measured values shown in Table 2, which are the total ice weight collected on the blowing and nonblowing sections of the model. Details of the computation are given in the following section.) The effect of nonuniform injection, i.e., different flow rate through each slot, was examined next, keeping all other parameters constant. The flow through slots 1 and 3 (+50 and −50 deg, respectively) was set at 100 ft^3/h and through slot 2 (at stagnation point) at 150 ft^3/h, which produced 1.42 g of ice. Other injection rates were also used, and the results are presented in Tables 2 and 3.

In Figs. 7–9, the angular ice profiles for the case of surface injection are compared to those with no surface injection. The effects of injection are clearly shown by the reduction in the area under each curve. The approximate location of the slot(s) is marked on these curves. The extent of ice reduction can also be observed if one compares these profiles with the axial ice profile shown in Fig. 6. The angular ice profiles indicate that

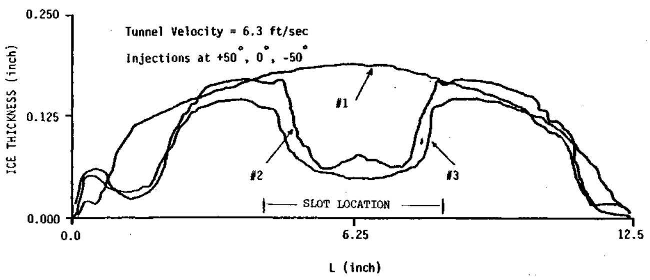

Fig. 6 Axial ice profiles along the cylinder at $\theta = +5$ deg from the front stagnation point. Injection rates at the slots: curve 1 = 0, 0, 0; curve 2 = 0, 200, 0; curve 3 = 100, 200, 100 (ft^3/h).

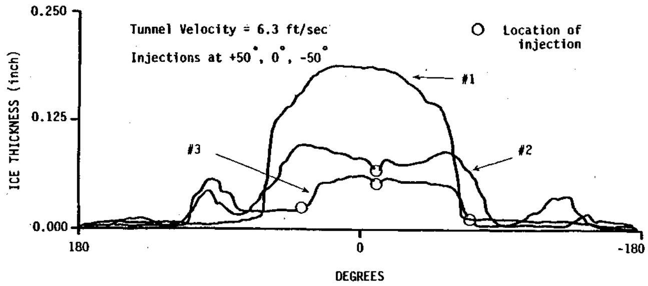

Fig. 7 Angular ice profiles around the cylinder at 1.25 in. to the right of the center of the cylinder. Injection rates correspond to those of Fig. 6.

Table 2 Experimental ice weights collected on the model, set 1

		Air injection flow rate, ft^3/h				Room air temperature, °F		
Run[a]	Tunnel speed, ft/s	Slot 1[b]	Slot 2	Slot 3	Run time, min	Dry bulb	Relative humidity	Ice weight, g
1	6.3	0	0	0	7	66	54	14.75
2	6.3	25	25	25	7	70	38	13.00[c]
3	6.3	100	100	100	7	68	51	12.75
4	6.3	100	150	100	7	64	45	11.25
5	6.3	50	150	50	7	70	38	13.80
6	6.3	50	0	50	7	70	38	9.80
7	6.3	100	0	100	7	71	35	8.30
8	6.3	0	200	0	7	71	50	9.60
9	6.3	0	50	0	7	72	46	11.60
10	6.3	100	200	100	7	71	35	9.30

[a]Test no. [b]Location of slots 1, 2, 3: +50, 0, −50 from the front stagnation point. [c]Slot clogging experienced.

Table 3 Experimental ice weights collected on the model, set 2

		Air injection flow rate, ft^3/h				Room air temperature, °F		
Run[a]	Tunnel speed, ft/s	Slot 1[b]	Slot 2	Slot 3	Run time, min	Dry bulb	Relative humidity	Ice weight, g
1	13.3	0	0	0	7	70	30	22.63
2	13.3	100	100	100	7	70	24	19.00
3	13.3	0	200	0	7	70	27	20.80
4	13.3	100	200	100	7	80	45	22.00
5	13.3	100	0	100	7	80	45	21.30
6	13.3	50	150	50	7	80	45	21.60
1	39.0	0	0	0	7	68	35	42.30
2	39.0	100	200	100	7	70	34	40.30[h]
1	4.1	0	0	0	7	70	34	7.90
2	4.1	100	100	100	7	70	34	7.00

Footnote definitions as in Table 2.

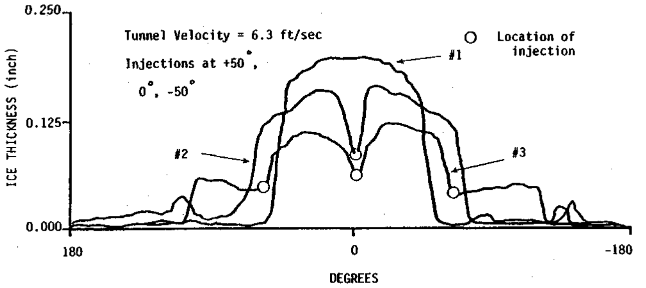

Fig. 8 Angular ice profiles around the cylinder at the center of the cylinder. Injection rates correspond to those of Fig. 6.

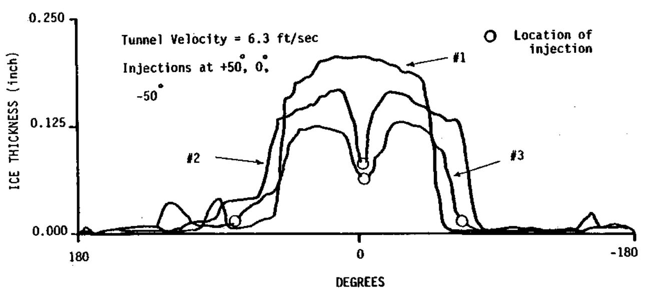

Fig. 9 Angular ice profiles around the cylinder at 1.25 in. to the left of the center of the cylinder. Injection rates correspond to those of Fig. 6.

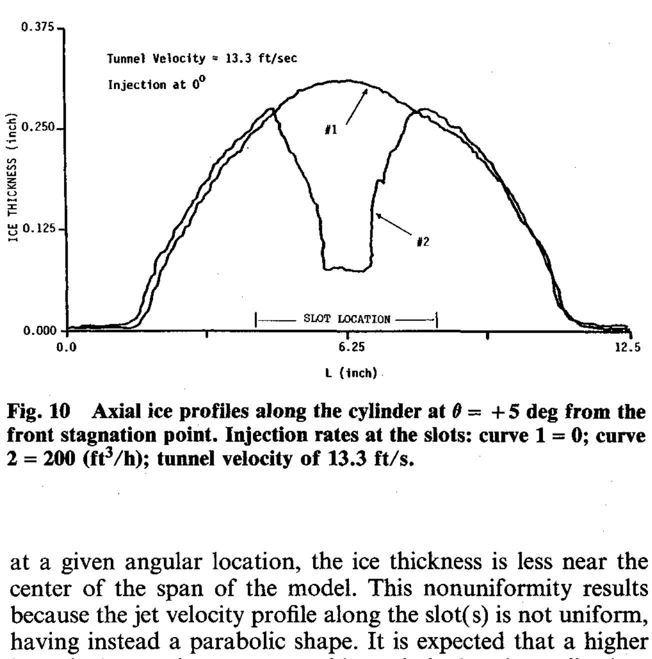

Fig. 10 Axial ice profiles along the cylinder at $\theta = +5$ deg from the front stagnation point. Injection rates at the slots: curve 1 = 0; curve 2 = 200 (ft^3/h); tunnel velocity of 13.3 ft/s.

at a given angular location, the ice thickness is less near the center of the span of the model. This nonuniformity results because the jet velocity profile along the slot(s) is not uniform, having instead a parabolic shape. It is expected that a higher jet velocity at the center would result in less ice collection, which is indicated by the ice profile at the center. More ice is collected under a higher tunnel velocity (13.3 ft/s), as indicated by Figs. 10 and 11, with the tunnel liquid water content and the mean droplet diameter the same as in the previous case. The increase in ice accretion is due to the higher droplet inertia and its slow response to the changes in the flow conditions. Streamlines are closer to the surface and have sharper gradients near the surface, and more droplets are separated from the streamlines and collected on the surface as compared with those of the slower tunnel velocity.

Figure 12 is a sketch of typical ice shapes obtained in the experiments. These shapes are not necessarily typical of those found in actual icing situations (see Fig. 1) since the freezing mechanism of the droplets collected on the surface was different from that of the actual atmospheric icing.

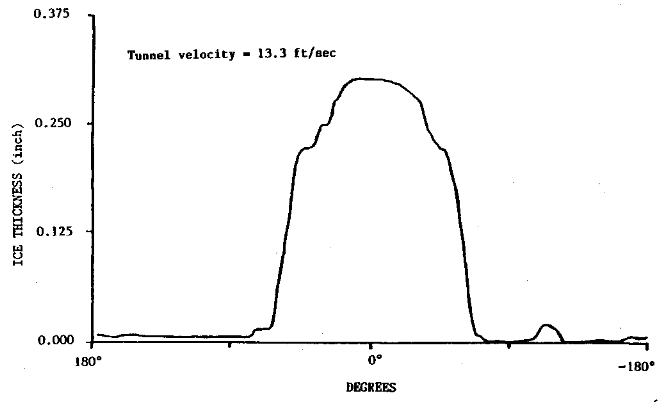

Fig. 11 Angular ice profile around the cylinder at the center of the cylinder; tunnel velocity of 13.3 ft/s.

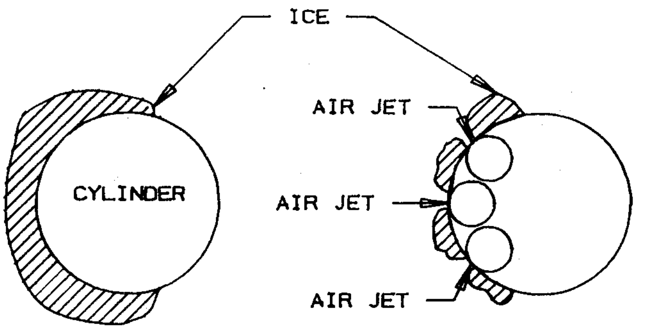

Fig. 12 Sketch of the typical ice shapes obtained experimentally on the cylinder.

Discussion of Results

A reduction in collected ice weights was realized in all tests conducted when injection was used. It is important, however, to keep in mind that slot injection increases the effective blockage of the test section (jets opposing the main flow), thereby causing a redistribution of the flow in the remaining region of the test section. Therefore, compared to the case of no injection, higher velocities were realized over the model when injection was taking place. The collection efficiency of the model is higher for a higher velocity due to the increase in inertia of the droplets and their subsequent separation from the streamlines near the cylinder, as explained previously. Thus, the ice weights obtained with injection are generally higher than those for a larger test section since the blockage effects due to injection are negligible.

The effect of room air humidity on the collected ice weight can be seen from the results of runs obtained with a tunnel velocity of 13.3 ft/s. Run 4, which corresponds to a higher injection rate than those in runs 2 and 3, actually results in more ice collection than in those runs. This increase in ice weight is due to the higher humidity of room air. The room air humidity was 20% for runs 2 and 3 and 45% for run 4. Thus, the ice weights of runs 4–6 cannot be directly compared with those of runs 1–3.

Percent reduction in the collected ice mass due to surface blowing was determined by estimating an average ice weight collected per unit length of the blowing surface. Average ice weight on the unslotted section of the model was calculated by assuming that the thickness of the ice collected on the model, with no surface injection, is uniform. Furthermore, assuming that the effect of blowing is confined to the slotted section of the model, ice weight collected on the unslotted section of the model for the blowing and nonblowing cases would be the same. This weight was then subtracted from the ice weights shown in Tables 2 and 3 to obtain the ice weight collected on the blowing section (ice weights shown in Tables 2 and 3 are the combined weights of the accreted ice over the blowing and nonblowing sections of the model). The percentage reductions in the accreted ice weight per unit length are estimated and are as follows. For tunnel speed of 6.3 ft/s, runs 6–8 and 10 indicate about 100% reduction in ice. However, this was not the case, as indicated by the ice profiles shown in Figs. 6–9. Run 5 has about 18% reduction, which is the minimum for this particular tunnel speed. The reductions in ice for runs 2–4 and 9 is about 35, 40, 72, and 64%, respectively. For tests conducted with a tunnel speed of 13.3 ft/s, the maximum reduction is about 48%, corresponding to run 2, and the minimum reduction is about 7%, corresponding to run 4. The reduction for runs 3, 5, and 6 is about 23, 16, and 14%, respectively. Finally, the reductions in ice for run 2 with tunnel speeds of 39 and 4.1 ft/s are about 17 and 15%, respectively.

A general correlation for the ice accretion rate on a blowing surface can be formulated without considering the limitations discussed earlier. The rate of ice accretion is reduced with an increase in total surface injection rate. An increased number of injection slots results in lesser ice accretion than a single-slot model with the same total injection rate.

Concluding Remarks

The experimental results indicate a general reduction in ice accretion rate due to slot injection. The ice accretion is a nonlinear function of the tunnel speed and increases with that speed; the decrease in accretion rate is a nonlinear function of the injection rate. No empirical correlation of the results was obtained due to experimental limitations and problems encountered.

Better results could be achieved if a more uniformly distributed droplet flow were produced with uniform droplet size. Also, a larger tunnel test section could reduce the three-dimensional effects. An increase in the number of slots could definitely reduce the ice collection even further than was experienced with only three slots. Finally, to minimize the three-dimensional effects caused by nonuniform axial velocity at the exit of slots, a porous model surface is recommended.

Additionally, parametric studies are needed to vary slot number, location, and width along with the ratio of slot velocity to freestream velocity. Also, in any further testing, a two-phase wind tunnel should be used so that the air humidity and temperature can be carefully controlled.

References

[1]Laschka, B. and Jesse, R., "Ice Accretion and Its Effects on Aerodynamics of Unprotected Aircraft Components," AGARD Advisory Rept. 127, Nov. 1978.

[2]Stallabrass, J. R., "The Icing of an Unheated Non-Rotating Cylinder in Liquid Water Droplet-Ice Crystal Clouds," Report of the National Research Council of Canada, Feb. 1979.

[3]Brun, E. A., "Icing Problems and Recommended Solutions," *AGARDograph* 16, Nov. 1957.

[4]Keshock, E. G., Missimer, J. R., and Tabrizi, A. H., "Scaling Analysis of the Ice Accretion Process on Aircraft Surfaces," American Society of Mechanical Engineers Paper WA-HT-39, Jan. 1982.

[5]Armand, C., "Techniques and Facilities Used at the Onera Modane Center for Icing Tests," AGARD Advisory Rept. 127, Nov. 1978.

[6]Lake, H. B. and Bradley, J., "The Problem of Certifying Helicopters for Flight in Icing Conditions," *Aeronautical Journal*, Vol. 80, Oct. 1976, pp. 419–433.

[7]Potapczuk, M., "Numerical Analysis of a NACA 0012 Airfoil with Leading Edge Ice Accretions," AIAA Paper 87-0101, Jan. 1987.

[8]Scott, J. N., "Navier-Stokes Solution of the Flowfield Over Ice Accretion Shapes," AIAA Paper 12-5, Jan. 1987.

[9]Nichols, C. C., "Ice Protection of Engine Air Inlet for Cruise Missile Applications," American Society of Mechanical Engineers Paper ENAs-2, 1980.

[10]Kohlman, D. L., "Icing Tunnel Tests of a Glycol-Exuding Porous Leading Edge Ice Protection System on a General Aviation Airfoil," AIAA Paper 81-0405, Jan. 1981.

[11]Horne, A. T., "Weeping Wings," *AOPA Pilot*, Aircraft Owners and Pilot Association, Vol. 27, Jan. 1984, pp. 36–38.

[12]Hauger, H. H., "Intermittent Heating of Airfoils for Ice Protection Utilizing Hot Air," American Society of Mechanical Engineers Paper SA-42, March 1953.

[13]Leffel, K. L., "A Numerical and Experimental Investigation of Electrothermal Aircraft Deicing," *Proceedings of the 42nd Meeting of the American Helicopter Society*, Washington, DC, June 1986.

[14]Hung, C.-C., Dillehay, M. E., and Stahl, M., "A Heater Made From Graphite Composite Material for Potential Deicing Application," AIAA Paper 87-0025, Jan. 1987.

[15]Ciardullo, S. W., Mitchell, S. C., and Zerkle, R. D., "Evaluation of Capillary Reinforced Composites for Anti-Icing," AIAA Paper 87-0023, Jan. 1987.

[16]Tabrizi, A. H., "An Experimental and Theoretical Investigation of an Air Injection Type Anti-Icing System for Aircraft," Ph.D. Dissertation, The University of Tennessee, Knoxville, TN, 1986.

[17]Tabrizi, A. H. and Keshock, E. G., "Modeling of Surface Blowing From Discrete Slots as a Mechanism for Preventing Ice Accretion on Aircraft Surfaces," AIAA Paper 87-0026, Jan. 1987.